Observation of Polarization-Locked Vector Solitons in an Optical Fiber

S. T. Cundiff,[1] B. C. Collings,[2,3] N. N. Akhmediev,[4] J. M. Soto-Crespo,[5] K. Bergman,[2] and W. H. Knox[3]
[1]*JILA, University of Colorado and National Institute of Standards and Technology, Boulder, Colorado 80309-0440*
[2]*Department of Electrical Engineering, Princeton University, Princeton, New Jersey 08544*
[3]*Bell Labs, Lucent Technologies, Holmdel, New Jersey 07733*
[4]*Australian Photonics Cooperative Research Centre, Optical Sciences Centre, The Australian National University, Canberra, ACT 0200, Australia*
[5]*Instituto de Óptica, Consejo Superior de Investigaciones Cientificas, Serrano 121, 28006 Madrid, Spain*
(Received 8 December 1998)

We observe polarization-locked vector solitons in a mode-locked fiber laser. Temporal vector solitons have components along both birefringent axes. Despite different phase velocities due to linear birefringence, the relative phase of the components is locked at $\pm\pi/2$. The value of $\pm\pi/2$ and component magnitudes agree with a simple analysis of the Kerr nonlinearity. These fragile phase-locked vector solitons have been the subject of much theoretical conjecture, but have previously eluded experimental observation. [S0031-9007(99)09109-7]

PACS numbers: 42.81.Dp, 05.45.Yv

The observation of temporal solitons in optical fiber [1] has resulted in a huge amount of research. This has been motivated by both fundamental interest and the potential for applications in telecommunications. Despite the fact that "single" (radial) mode optical fiber supports two orthogonal polarization modes, soliton propagation in optical fiber is often treated as a scalar problem, and the vector nature of light is ignored [2]. Although this would be valid if the fiber were truly isotropic, in reality it is always slightly birefringent due to strain, bends, etc. The presence of birefringence lifts the degeneracy between the two modes, resulting in coupling and differing phase and group velocities. Because of differing phase velocities, the soliton polarization will evolve as it propagates. A differing group velocity causes the energy propagating in each mode to temporally separate, destroying the soliton. Clearly, the very observation of solitons in fiber implies that the group velocity of the modes lock together. This occurs via a slight shift in the frequencies of the two orthogonal components, which shifts their group velocities, and has been the subject of both theory and experiment [3,4]. Normally, the polarization state of solitons propagating through low birefringence fiber remains uniform across the pulse but evolves with position [4,5].

For solitons to propagate with a uniform, nonevolving polarization state, the phase velocities must lock. This was also predicted, resulting in a soliton that preserves its polarization state in the presence of birefringence. However, phase velocity locking is more difficult to obtain than group velocity locking because the phase velocity difference is larger in standard fiber. Furthermore, since the birefringence of standard single mode fiber is generally randomly distributed and propagation over long distances is accompanied by losses, experimental study of polarization-locked solitons in transmission systems is difficult. Here, we report the observation of such polarization-locked vector solitons (PLVS) in a mode-locked fiber laser. This mode-locked fiber laser provides a unique system that is nearly conservative, has well-controlled birefringence, and allows monitoring of the pulse during propagation over an essentially infinite distance. This makes it well suited for observing vector solitons in a controlled environment.

The use of temporal vector solitons for communications [4] and all-optical switching [6] has been explored. Recently, the nonlinear polarization evolution of solitons has been shown to differ significantly from linear propagation in standard low-birefringence fiber [7]. These experiments in a relatively short, very low loss, fiber provided evidence for instability of the fast axis and that some elliptically polarized states are preferred.

A full vector description of the soliton requires the use of coupled-nonlinear Schrödinger equations that describe the evolution of the polarization components along the two principal axes of the fiber [3,8,9]

$$iu_z + i\delta u_t + \gamma u + \tfrac{1}{2}u_{tt} + (|u|^2 + A|v|^2)u + Bv^2u^* = R_1(u,v,z,t),$$

$$iv_z - i\delta v_t - \gamma v + \tfrac{1}{2}v_{tt} + (|v|^2 + A|u|^2)v + Bu^2v^* = R_2(u,v,z,t),$$

where u and v are the envelope components along the principal axes, z and t are normalized time and distance, 2δ is the group velocity difference, 2γ is the phase velocity difference, A is cross-phase modulation coefficient, and B is the coefficient for coherent energy exchange (also known as four-wave mixing). In lossless media, $B = 1 - A$. All nonconservative effects are lumped into the right-hand side of the equations (R_1 and R_2). These are primarily gain and absorption, both of which may depend on time and pulse energy due to saturation. The aforementioned group velocity locking [3] means that, in the presence of weak, randomly varying birefringence,

 0031-9007/99/82(20)/3988(4)$15.00

the soliton polarization evolves as a unit [4]. Hence, the scalar approximation often provides an acceptable description of the envelope evolution.

We have studied the polarization evolution of solitons circulating in a mode-locked fiber laser and observed that PLVS form for low amounts of intracavity birefringence. For a PLVS, both u and v are nonzero and their relative phase is fixed. A PLVS uses the nonlinear phase shifts from self-phase modulation (SPM) and cross-phase modulation (XPM) to compensate for the differing phase velocities of u and v, much as an ordinary soliton uses SPM to cancel group-velocity dispersion. However, the PLVS is a much more fragile state than an ordinary soliton because it requires that the nonlinear phase shift for u or v dynamically adjust in response to external perturbations. Dynamic adjustment occurs via coherent energy exchange. Since the direction and magnitude of the energy flow due to coherent energy exchange is phase sensitive, perturbations cause adjustment in the relative amplitudes and thus the nonlinear phase shifts, thereby providing a negative feedback mechanism critical for stable phase locking.

Three solutions to the coupled nonlinear Schrödinger's equation result in solitons with a fixed polarization in low birefringence fiber. The first occurs when one axis becomes unstable. For a positive Kerr coefficient (as in optical fiber), the fast axis becomes unstable when the nonlinear contribution to its index of refraction causes its index to become larger than the slow axis. This has been described for both continuous-wave (cw) [10] and soliton propagation [11]; in the latter case, linearly polarized solitons along the slow axis result. Experimental evidence for soliton axis instability was recently observed [7]. A second solution to the coupled nonlinear Schrödinger's equation with fixed polarization occurs if the XPM coefficient, A, is equal to 1; then SPM and XPM are equal. This is known as the Manakov case. In isotropic material $A = \frac{2}{3}$, therefore this solution has only been observed in an anisotropic waveguide [12] where the relative strengths of SPM and XPM can be engineered to be approximately equal (i.e., $A \sim 1$). The third possibility is the PLVS. The general concept of a vector soliton was introduced by Christodoulides and Joseph [13]. However, their solution was later found to be unstable during propagation and decomposed into two solitons. A stable solution consisting of a single elliptically polarized soliton was analytically discovered later [14,15]. Recent numerical results [16] have found results corresponding to the analytical solutions, which assume a conservative system. We also note that in nonisotropic fiber, which has a high intrinsic birefringence (polarization preserving fiber), solitons typically occur only along one axis due to the strong group-velocity difference. In such fiber, the nonlinear index can never be comparable to the birefringence and, hence, the above discussion does not apply. Here, we restrict ourselves to the limit of low birefringence where it does apply.

Analytical approaches to solving the coupled nonlinear Schrödinger's equation usually assume a conservative system, i.e., one without gain or loss. Consequently, the solutions that they provide have limited applicability to typical fiber-optic transmission systems, where lumped optical amplification results in strong nonconservative perturbations as the pulse amplitude decays significantly before reamplification. To avoid this difficulty, we studied soliton propagation in a fiber laser, where the perturbations per round-trip are small. Although the fiber laser cavity is short (4 m round-trip), it is a very good experimental realization of an infinite, lossless transmission line. In addition, by using a fiber laser, we are able to observe the evolution of the soliton as it propagates because a small amount is coupled out of the cavity after each round trip. This is a significant advantage over experiments that simply propagate pulses through a fixed length of fiber and, hence, cannot observe the evolution with propagation distance. Furthermore, we need only to characterize a short length of fiber.

The experimental setup is shown in Fig. 1. The fiber laser consists of three pieces of single (spatial) mode fiber fusion spliced together. The 10 cm long center piece is erbium/ytterbium codoped to provide gain. This fiber has normal dispersion due to the small waveguide diameter. The other two pieces are standard fiber with anomalous dispersion. The net cavity dispersion is anomalous. One end of the cavity is butt coupled to a saturable-Bragg reflector [17], a monolithic semiconductor device that provides saturable absorption and serves as a high reflector. The saturable absorption starts and stabilizes the formation of ultrashort pulses. The other end of the cavity is a dielectric mirror coated directly onto the fiber. This mirror acts as an output coupler (~99% reflectivity at the lasing wavelength, $\lambda = 1550$ nm). The pulses formed in the cavity are fundamental solitons of the average cavity dispersion and nonlinearity. The erbium/ytterbium fiber is pumped with 980 nm light that is injected through the output coupler. A portion of single mode fiber making up the laser cavity is wrapped around two 5.5 cm diameter paddles of a fiber polarization controller [18]. With three wraps, each paddle provides just under $\lambda/4$ linear retardance. The remaining fiber in the cavity contributes a small amount of residual retardance (typically less than $\lambda/8$). By changing the angles of the two paddles, Θ_1 and Θ_2, we can adjust the total cavity retardance from zero to approximately a full wavelength. Although the birefringence magnitude

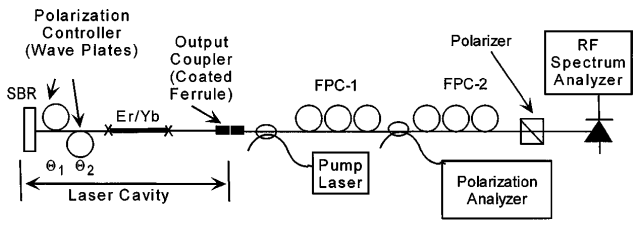

FIG. 1. Experimental setup; FPC is a fiber polarization controller.

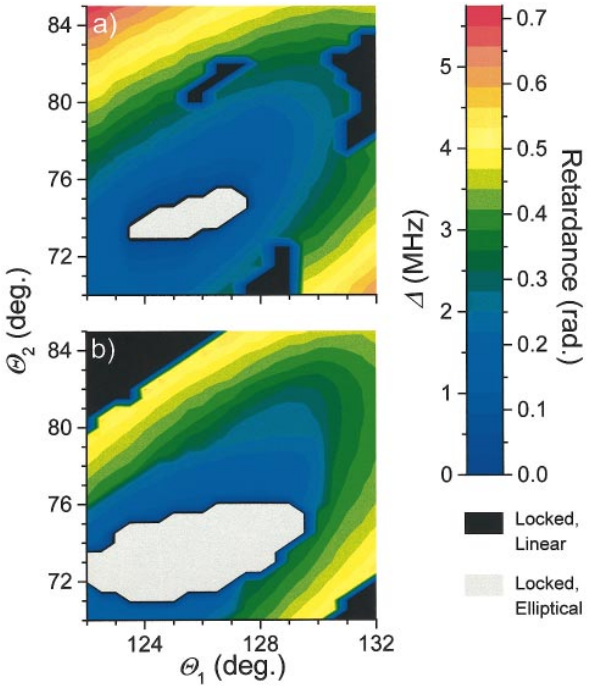

FIG. 2(color). Measured polarization evolution frequency, Δ, as a function of the angles of the intracavity polarization controllers, Θ_1 and Θ_2, for (a) high pulse energy and (b) low pulse energy. Colors represent Δ, which can be mapped into round-trip retardance (both are shown on the scale). Gray and black regions are where the polarization is locked.

and orientation of the axes varies within the cavity, this variation occurs on a length scale much shorter than the soliton period [2]; hence, the soliton responds only to the average birefringence. This is in contrast to transmission experiments where random changes occur on length scales long enough for the soliton to adjust adiabatically.

To measure the round trip retardance in the laser cavity, we pass the output through a linear polarizer and detect it with a fast photodiode [19]. The radio-frequency (rf) spectrum of the resulting electrical signal displays a harmonic comb spaced by the $1/\tau_c$, where τ_c is the cavity round-trip time ($\sim$20 ns). Each peak in the comb also has sidebands, with an amplitude that depends on the linear polarizer orientation, but a spacing that does not (typical data are shown in Ref. [19]). We call the frequency spacing, Δ, between the harmonic comb and the sidebands, the polarization evolution frequency (PEF). The round-trip birefringence, β, is related to Δ by $\beta = 2\pi\Delta\tau_C$ and γ by $\gamma = \pi\Delta\tau_C/l$, where l is the cavity length. In Fig. 2, Δ is plotted as a function of Θ_1 and Θ_2 for two different pulse energies (controlled by the pump power). The basic structure of this plot is determined by linear birefringence [19].

There are several regions in Fig. 2 where the polarization is locked (i.e., the sidebands vanish) for all orientations of the polarizer and settings of a second fiber polarization controller (FPC-2 in Fig. 2). These regions are indicated by gray or black. This behavior does not occur if the laser is operated cw. Comparing Figs. 2(a) and 2(b), it is clear that the size and positions of the locked regions depend on pulse energy. These two facts prove the locking arises from nonlinearity.

To determine which of the mechanisms described above causes the locking, we used a polarization analyzer to measure the output polarization in these regions. The first fiber polarization controller (FPC-1) compensates for the birefringence in the fiber between the output coupler and the polarization analyzer.

Measurement of the polarization shows that some of the locking regions are linearly polarized (denoted by black in Fig. 2) while others are elliptically polarized (gray in Fig. 2). A linearly polarized output state suggests the axis instabilities described above. To verify this, we must determine the orientation of the principal axes in the laser cavity. We do this by examining the rf spectrum for cw operation and adjusting the linear polarizer before the photodiode to null the PEF sideband, which occurs when the polarizer is aligned along a cavity principal axis. (FPC-2 is used to compensate for all birefringence between the laser and the polarizer.) This can be understood by decomposing the pulse into components along the principal axes of the cavity, which have slightly different indices and, hence, round-trip times. The polarization evolution, and, hence, the rf sidebands, arises from beating between the orthogonal components when both are sampled by the polarizer. Thus, when the polarizer is aligned along a cavity axis, the beating and sidebands vanish. This reveals that, in the black regions, the output is linearly polarized along a cavity axis, as shown in Fig. 3. However, no information is obtained about which axis is the fast axis. Furthermore, arguments about which axis is stable and modified by the periodicity of the laser cavity. Nevertheless, we confidently assign the black regions with a fixed, linearly polarized output to an axis instability.

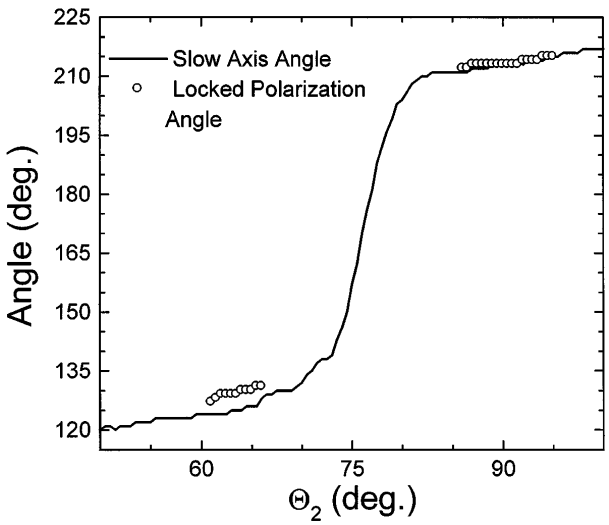

FIG. 3. Angles of the cavity axis and linearly polarized output versus paddle angle, Θ_2, for a fixed Θ_1 of 34°.

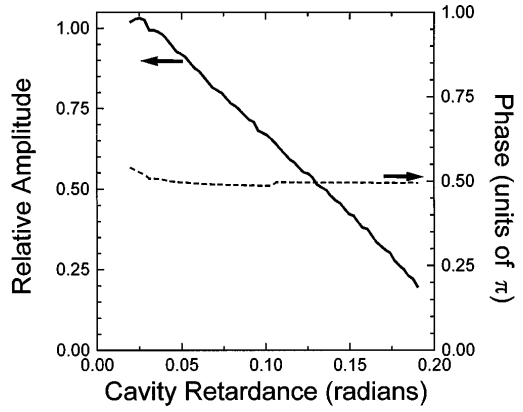

FIG. 4. Measured relative amplitude and phase of the components along the cavity principal axes versus total cavity retardance, β.

The elliptically polarized output observed in the gray regions in Fig. 2 has nonzero components along both principal axes, a requirement for a PLVS. To verify that the pulse is a PLVS, we completely characterize the polarization state by measuring both the amplitude of the components along the principal axes and relative phase. These parameters are obtained by transforming the polarization state measured by the polarization analyzer into the coordinate system of the cavity principal axes, which are measured as described above. The results, shown in Fig. 4, prove that the relative phase between the components is fixed at $\pi/2$, while the relative amplitudes vary with cavity retardance. The relative phase is bistable in that a phase of $-\pi/2$ is also observed [15].

To understand this, we examine how the combined effects of the nonlinear index of refraction (SPM and XPM) and coherent energy exchange compensate for the birefringence and stabilize the relative phase of the two components. The compensation of the birefringence is straightforward. If the power distribution between the two components is correct, the difference in their nonlinear indices renders the fiber effectively isotropic (the component along the fast axis must have higher relative power, which increases with increasing retardance). The calculated differential nonlinear phase shift based on the data in Fig. 4 agrees with the linear retardance, confirming that compensation occurs.

In addition to having the correct power distribution, there must be a mechanism for maintaining the precise distribution. Coherent energy exchange combined with the differential nonlinear phase shift provides such a mechanism. Coherent energy exchange is phase sensitive, it is zero for a $\pm\pi/2$ relative phase. Close to $\pm\pi/2$, it causes energy to be transferred to the component with advanced phase. This energy transfer causes the nonlinear index of that component to increase, thereby reducing its phase velocity. The reduction in phase velocity corrects the initial advanced phase. This combination of effects provides a negative feedback mechanism that stabilizes the relative phase at $\pm\pi/2$ and the relative intensities such that the differential nonlinear index for each component compensates the linear birefringence. Therefore a steady state situation will occur for a relative phase of $\pm\pi/2$, exactly what our measurements show. The results in Fig. 4 therefore constitute proof that a PLVS exists in the laser cavity.

Since the smaller component of the PLVS is along the slow axis, we can identify the fast axis within the PLVS region. By carefully tracking the axes as we adjust Θ_1 and Θ_2 away from the PLVS regions and into a linearly locked region, we confirm that the linearly locked output is aligned along the slow axis. This confirms that these regions result from the fast axis instability. This measurement provides a more convincing demonstration of the fast axis instability than the earlier measurements [7].

In summary, we have experimentally observed phase-locked temporal vector solitons in optical fiber. These solitons have been the subject of substantial theoretical work. We are able make these observations by using a low perturbation fiber laser, which provides a good approximation to a conservative system.

[1] L. F. Mollenauer, R. H. Stolen, and J. P. Gordon, Phys. Rev. Lett. **45**, 1095 (1980).
[2] G. P. Agrawal, *Nonlinear Fiber Optics* (Academic Press, San Diego, 1989), 2nd ed.
[3] C. R. Menyuk, Opt. Lett. **12**, 614 (1987).
[4] S. G. Evangelides *et al.*, J. Lightwave Technol. **10**, 28 (1992).
[5] M. N. Islam *et al.*, Opt. Lett. **15**, 21 (1990).
[6] M. N. Islam, Opt. Lett. **14**, 1257 (1989).
[7] Y. Barad and Y. Silberberg, Phys. Rev. Lett. **78**, 3290 (1997).
[8] G. P. Agrawal, *Nonlinear Fiber Optics* (Academic Press, San Diego, 1995), 2nd ed.
[9] N. N. Akhmediev and A. Ankiewicz, *Solitons, Nonlinear Pulses and Beams* (Chapman and Hall, London, 1997).
[10] H. G. Winful, Opt. Lett. **11**, 33 (1986).
[11] K. J. Blow, N. J. Doran, and D. Wood, Opt. Lett. **12**, 202 (1987).
[12] J. U. Kang *et al.*, Phys. Rev. Lett. **76**, 3699 (1996).
[13] D. N. Christodoulides and R. I. Joseph, Opt. Lett. **13**, 53 (1988).
[14] N. N. Akhmediev, A. Buryak, and J. M. Soto-Crespo, Opt. Commun. **112**, 278 (1994).
[15] N. N. Akhmediev *et al.*, J. Opt. Soc. Am. B **12**, 434 (1995).
[16] N. N. Akhmediev *et al.*, Opt. Lett. **23**, 852 (1998).
[17] B. C. Collings *et al.*, IEEE J. Sel. Top. Quantum Electron. **3**, 1065 (1997).
[18] H. C. Lefevre, Electron. Lett. **16**, 778 (1980).
[19] S. T. Cundiff, B. C. Collings, and W. H. Knox, Opt. Ex. **1**, 12 (1997).